Date: July 23, 2020

Submitted to: *Bioresource Technology*, special issue

Impact of external resistance acclimation on charge transfer and diffusion resistance in bench-scale microbial fuel cells

Ruggero Rossi[1], Bruce E. Logan[1]*

[1]Department of Civil and Environmental Engineering, Penn State University, University Park, PA 16802, USA

*Corresponding author. Email: blogan@psu.edu

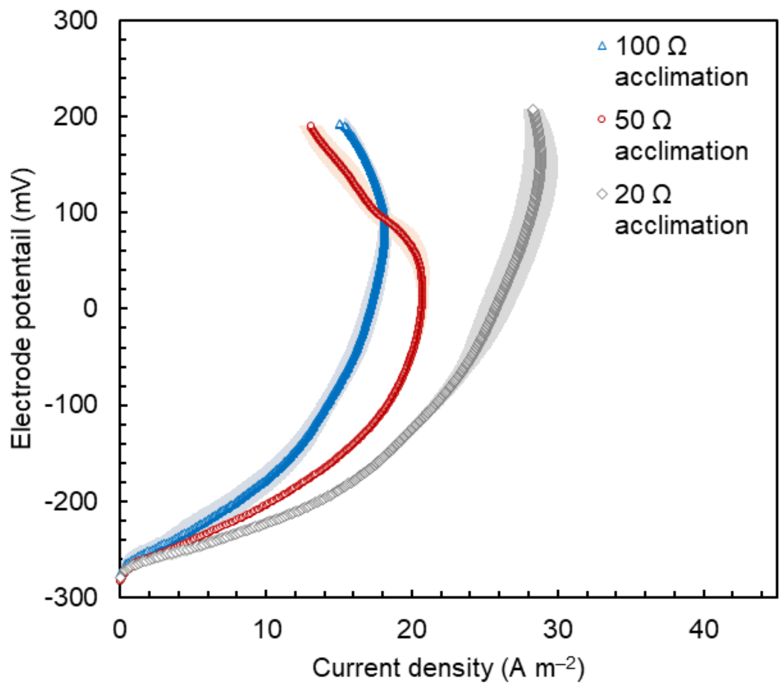

Figure S1: LSVs of carbon brush anodes acclimated at different external resistances not corrected for the solution resistance.

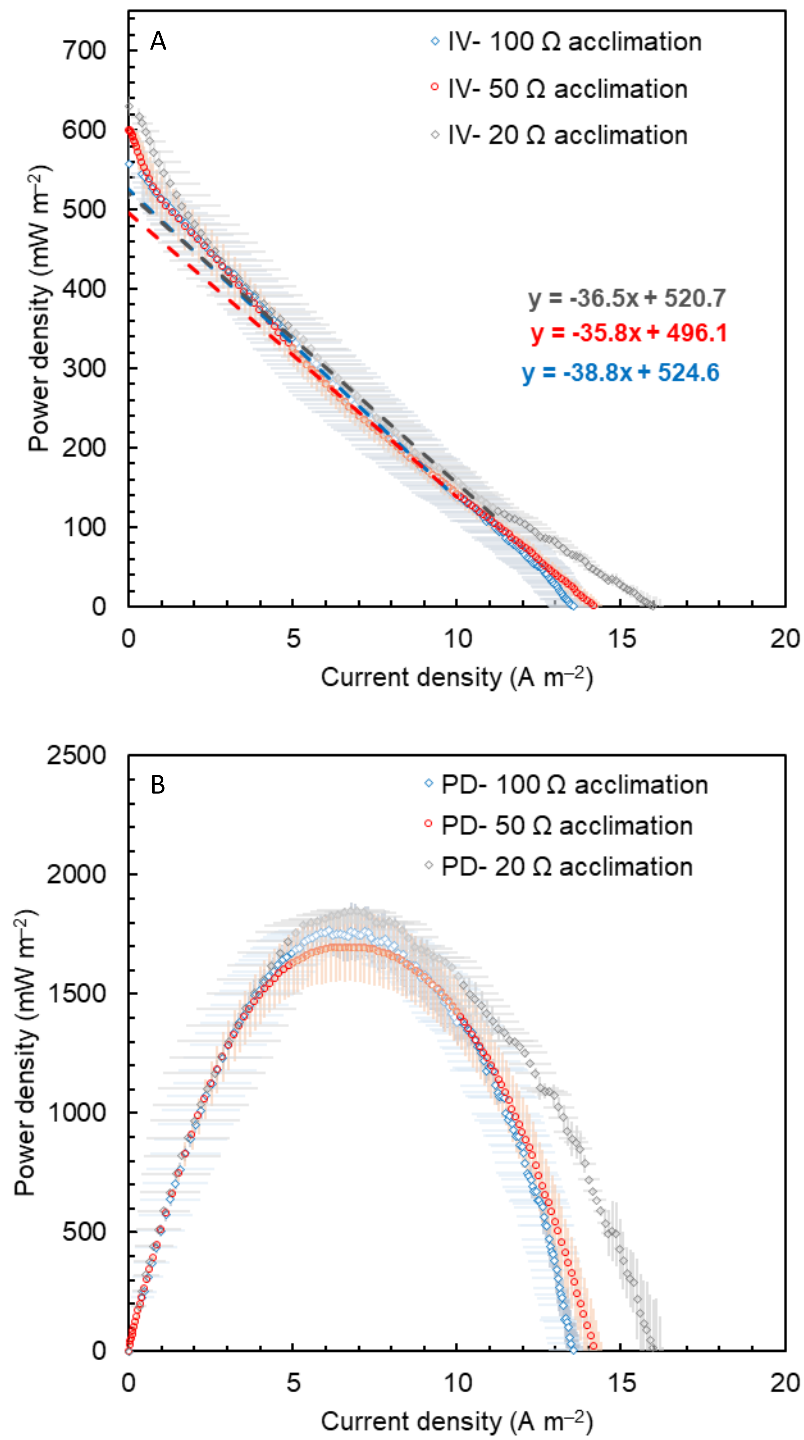

Figure S2. (A) Polarization and (B) power density curves of MFCs acclimated at an external resistance of 100 Ω, 50 Ω and 20 Ω.

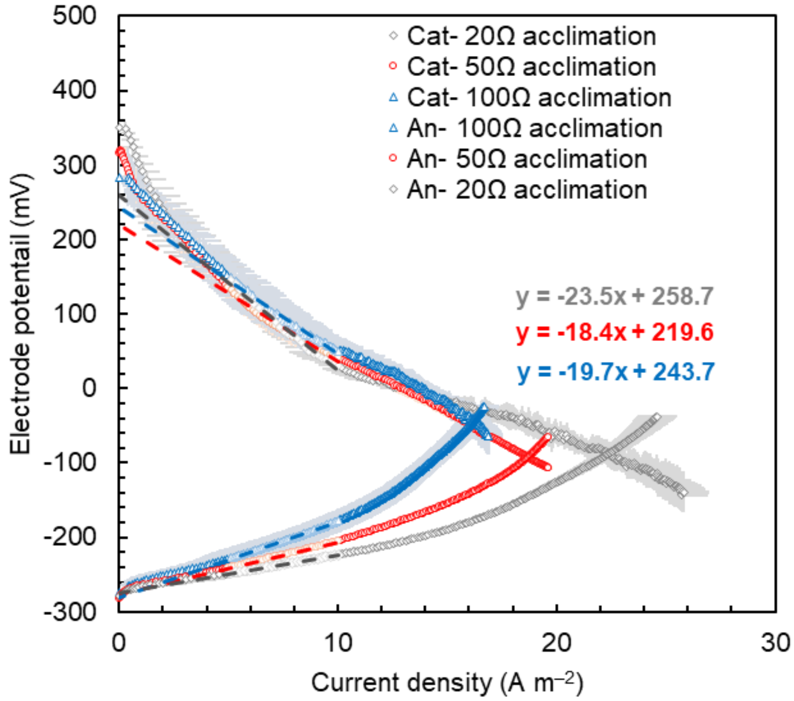

Figure S3. Anode and cathode electrode potentials from polarization curves of MFCs acclimated at an external resistance of 100 Ω, 50 Ω and 20 Ω.

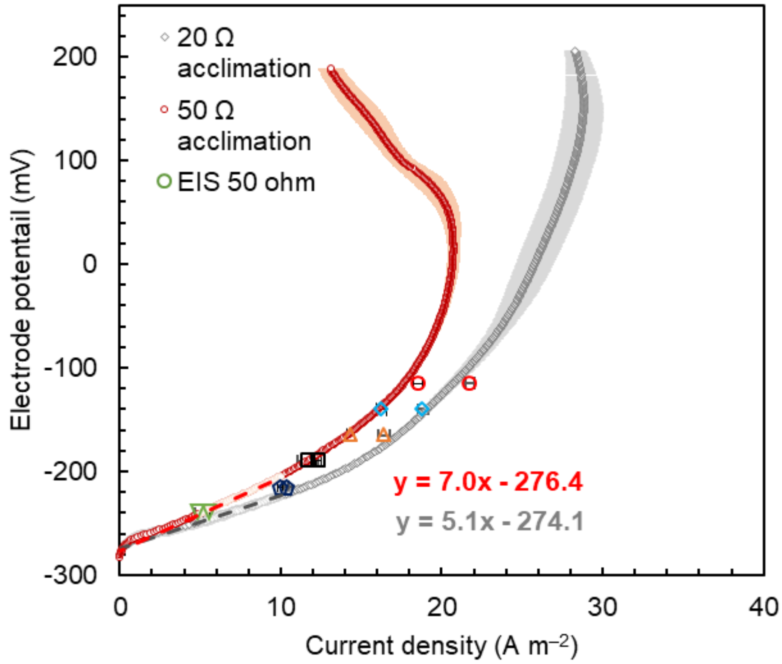

Figure S4. Comparison between the current density obtained at the correspondent anode potentials with 20 Ω and 50 Ω acclimated electrodes with LSVs with a scan rate of 0.1 mV s^{-1} and in EIS experiments at a fixed electrode potential.

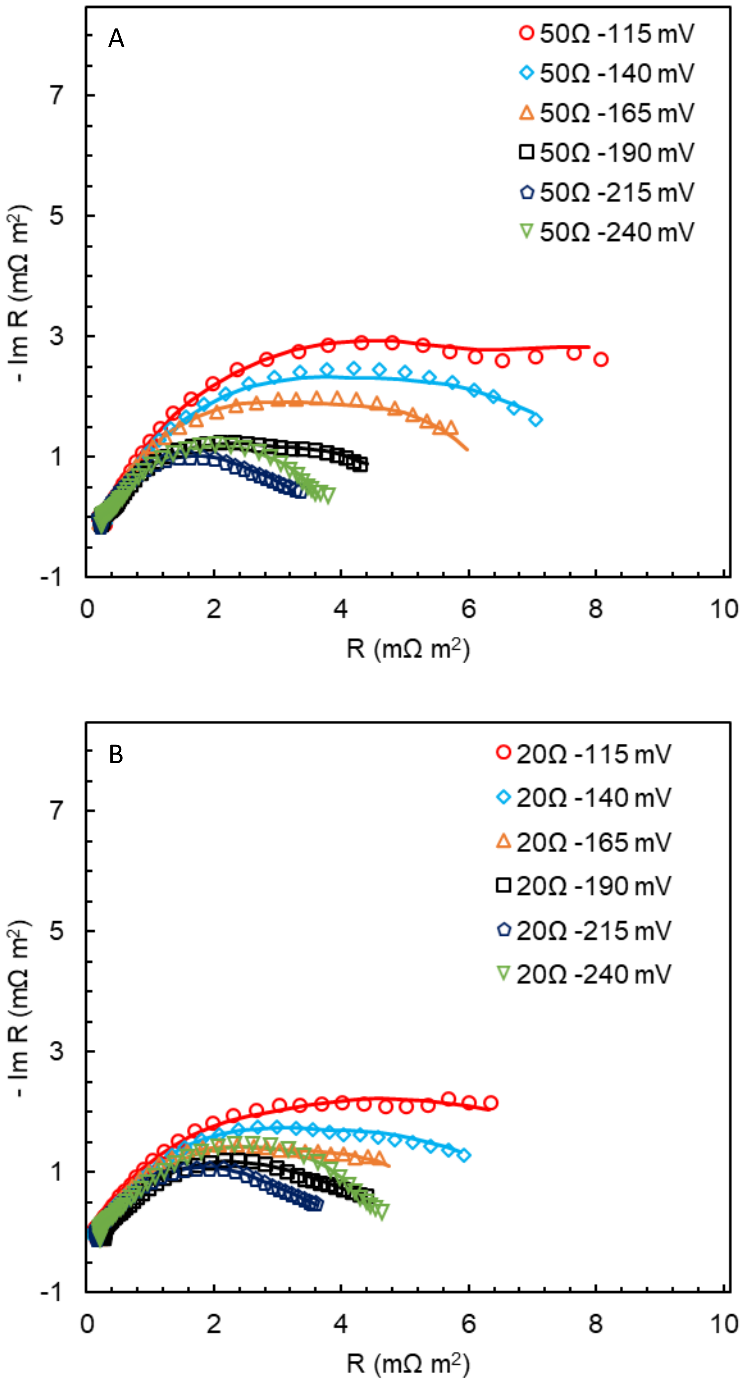

Figure S5: EIS spectra of anodes acclimated at (A) 50 Ω and (B) 20 Ω external resistances. Solid lines represent the fitting to the data.

Anode equivalent circuit. The anode spectrum is usually complicated by the presence of three different interfaces with the electrolyte: the biofilm, the graphite carbon bristles and the titanium current collector. Each of these elements have a characteristic frequency and can be present on the spectra as a distinct element. The spectra showed an inductive element (L_2/R_2) at high frequencies, likely due to the large capacitance of the coaxial cables used in the electrochemical setup or to artifacts from the RE which are not an integral part of the MFC (Brandstätter et al., 2016; Pivac and Barbir, 2016; Veal et al., 2015). Following the inductive element, solution resistance (between RE and electrode) and porosity solution resistance (Q_4/R_4) were identified. The Q_4/R_4 element was likely due to the small porosity of the graphite fibers, as its capacitance and resistance were independent by the applied potential and consequently, not involved in the electrochemical reaction (Ahn and Tatarchuk, 2006). The elements dominating the spectra were due to the anodic oxidation of acetate by the bacteria ($Q_{DL}/R_{CT}/(L_6+R_6)$, $Q_{DL}/(R_{CT}+Z_d)/(L_6+R_6)$), with capacitance ($Q_{DL}$) strictly related to the elctrode surface area and resistance connected to reaction kinetic and diffusion resistances ($R_{CT}+Z_d$). Induction was present at low frequencies (L_6+R_6) as it was previously reported in other studies using different configurations (Sevda et al., 2015). Inductance is defined as the property of an electric circuit to develop an electromotive force due to a change in the current passing through the system itself (Rossi et al., 2020). Inductance at low frequency have been identified with a change in the resistance of the electrochemical process over time (Klotz, 2019) and depending on the relative time of the change in the resistance in respect to the time constant of the electrochemical process a low frequency inductance could appear in the complex plane plots. These phenomena have been identified with side reactions with intermediate species (Pivac and Barbir, 2016), catalyst poisoning (Pivac and Barbir, 2016), wettability of the ion exchange membrane (Klotz, 2019; Roy et al., 2007) but also with experimental artifacts (Brandstätter et al., 2016). As the anodic electron transfer in bioelectrochemical system involves several multi-step reactions (Strycharz et al., 2011), it is likely that in our system, the induction is likely due to a two-step reaction, with the first reaction having a larger time constant than the consecutive ones.(Klotz, 2019)

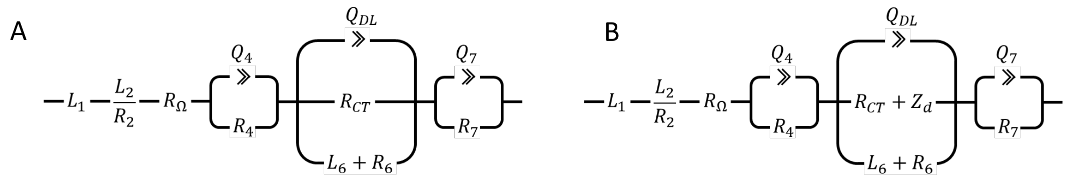

Figure S6. Equivalent circuit used to fit the impedance diagrams of the anodes (A) without and (B) with diffusion resistance recorded at different overpotentials.

Literature cited

1. Ahn, S., Tatarchuk, B.J., 2006. Air electrode: identification of intraelectrode rate phenomena via AC impedance. J. Electrochem. Soc. 142, 4169. https://doi.org/10.1149/1.2048480
2. Brandstätter, H., Hanzu, I., Wilkening, M., 2016. Myth and reality about the origin of inductive loops in impedance spectra of lithium-ion electrodes - A critical experimental approach. Electrochim. Acta 207, 218–223. https://doi.org/10.1016/j.electacta.2016.03.126
3. Klotz, D., 2019. Negative capacitance or inductive loop? – A general assessment of a common low frequency impedance feature. Electrochem. commun. 98, 58–62. https://doi.org/10.1016/j.elecom.2018.11.017
4. Pivac, I., Barbir, F., 2016. Inductive phenomena at low frequencies in impedance spectra of proton exchange membrane fuel cells – A review. J. Power Sources 326, 112–119. https://doi.org/10.1016/j.jpowsour.2016.06.119
5. Rossi, R., Hall, D.M., Wang, X., Regan, J.M., Logan, B.E., 2020. Quantifying the factors limiting performance and rates in microbial fuel cells using the electrode potential slope analysis combined with electrical impedance spectroscopy. Electrochim. Acta 348, 136330. https://doi.org/10.1016/j.electacta.2020.136330
6. Roy, S.K., Orazem, M.E., Tribollet, B., 2007. Interpretation of low-frequency inductive loops in PEM fuel cells. J. Electrochem. Soc. 154, B1378. https://doi.org/10.1149/1.2789377
7. Sevda, S., Chayambuka, K., Sreekrishnan, T.R., Pant, D., Dominguez-Benetton, X., 2015. A comprehensive impedance journey to continuous microbial fuel cells. Bioelectrochemistry 106, 159–166. https://doi.org/10.1016/j.bioelechem.2015.04.008
8. Strycharz, S.M., Malanoski, A.P., Snider, R.M., Yi, H., Lovley, D.R., Tender, L.M., 2011. Application of cyclic voltammetry to investigate enhanced catalytic current generation by biofilm-modified anodes of Geobacter sulfurreducens strain DL1 vs. variant strain KN400. Energy Environ. Sci. 4, 896–913. https://doi.org/10.1039/c0ee00260g
9. Veal, B.W., Baldo, P.M., Paulikas, A.P., Eastman, J.A., 2015. Understanding artifacts in impedance spectroscopy. J. Electrochem. Soc. 162, H47–H57. https://doi.org/10.1149/2.0791501jes